ISSN 1027-5495. Functional Materials, 23, No.2 (2016), p. 249-254.
doi:http://dx.doi.org/10.15407/fm23.02.249

Modification of sintered iron properties by Y_2O_3 nanoparticles

M.I.Cherednyk, O.Yu.Popov, S.V.Chornobuk, I.M.Totsky, M.P.Semenko, O.I.Boshko, V.Ja.Tkachuk, Y.V.Slobodianyk, S.M.Naumenko, V.A.Makara

Department of Physics of Metals, Faculty of Physics, T.Shevchenko National University of Kyiv, 4 Glushkova Ave., 03680 Kyiv, Ukraine

Received March 12, 2015

Influence of Y_2O_3 nanoparticles on sintered iron structure and microhardness is investigated. Ferrite grain growth is shown to be slowed down by the clusters which cause altering the grain shape from needle-like to equiaxial (with lower specific surface). Yttrium oxide particles resulted microhardness increasing to 3.6 GPa at 1 % of second phase content. The fact is explained by retardation of dislocations on disperse particles by the Orowan mechanism.

Keywords: powder metalurgy, yttrium oxide, steel, microhardness, structure.

Исследовано влияние наночастиц Y_2O_3 на структуру и микротвердость спеченного железа. Показано, что рост зерен феррита замедляется кластерами, которые вызывают изменение формы зерна из игольчатого на более равноосный. Добавление частиц оксида иттрия увеличивает микротвердость материала до 3,6 ГПа при 1 % содержании Y_2O_3. Данный факт объясняется торможением дислокаций об нанодисперсные частицы по механизму Орована.

Модифікація властивостей спеченого заліза наночастинками Y_2O_3. *М.І.Чередник, О.Ю.Попов, С.В.Чорнобук, І.М.Тоцький, М.П.Семенько, О.І.Бошко, В.Я.Ткачук, Є.В.Слободяник, С.М.Науменко, В.А.Макара.*

Досліджено вплив наночастинок Y_2O_3 на структуру і мікротвердість спеченого заліза. Показано, що зростання зерен фериту сповільнюється кластерами, які викликають зміну форми зерна з голчастого на більш рівноосний. Додавання частинок оксиду ітрію збільшує мікротвердість матеріалу до 3,6 ГПа при 1 % домішки Y_2O_3. Даний факт пояснюється гальмуванням дислокацій об нанодисперсні частинки за механізмом Орована.

1. Introduction

Oxide-dispersion strengthened (ODS) steels are promising materials with highly improved physical-mechanical characteristics [1]. Adding of 0.3–0.5 weight % yttria to steel improves its strength by 50 % and yield stress by 30–40 % [2]. It is also known [3] that radiation swelling resistance of the ODS steels is 2.5 times as high as that of conventional ones. Thus oxide contain steels are attractive structural materials for nuclear reactors [1–6].

Steels can be strengthen with many different oxides from which the most popular are zirconia, yttria and titania. However Y_2O_3 is more promising in regards of radiation stability. E.g. the authors of [4] concluded Y_2O_3 particles to be stable after 590 MeV proton irradiation, Cayron with coauthors [5] showed that yttria clusters don't dissolve in iron matrix at neutron irradiation up to 20 dpa while Voevodin et al. [6] proved its radiation swelling to be by a factor of ten slower than that of alumina.

It is well known [7] that mechanical characteristic of degradation under irradiation is caused by formation of a great amount of point defects which prevent dislocation movement and embrittle material. Modeling provided in [7] showed that at high temperatures the defects can disappear in sinks. J.Brodrick et al. [4] considering Y_2O_3 nanoparticles to be such sinks, modeled behavior of interstitials and vacancies near the clusters, and showed them being able to attract both due to stresses appearing as a result of matrix-inclusion lattice discrepancy.

Another factor of oxide particle on the steel radiation stability impact as it is mentioned in [8] can be matrix fine structure formation. Such structure contains a great amount of grain boundaries which as well are efficient defect sinks. Influence of yttria nanoparticles on ferrite nucleation and growth was investigated in [9]. It was shown that increasing of Y_2O_3 content leaded to laminated ferrite amount decreasing. However investigated yttria fraction was not more than 0.02 % while most authors [1–5, 7, 11] insisted on optimum oxide inclusion content within 0.1–1 %.

ODS-steels presented in many resent works [4, 10–12] were synthesized in two stages: i. mechanical one basing on milling of $Fe–Y_2O_3$ powder mixture to dissolve oxide particles in matrix; ii. hot isostatic pressing of obtained powder at a pressure up to 1 GPa.

The present work is an attempt to create iron-based material with yttria nanoparticles via conventional single-stage hot pressing of relevant powder mixtures and investigate oxide particle influence on structure and microhardness of sintered materials.

2. Experimental

Commercially available powders of carbonyl iron P-10 (2–5 μm, "Novohim" Ltd., Kharkiv, Ukraine) and monoclinic Y_2O_3 (40–60 nm, Novosibirsk State University, Novosibirsk, Russia) were used as starting materials. Different powder compositions (Table) were mixed in a planetary mill with rotation frequency 120 s^{-1} during 15 min. The powder mixtures were hot-pressed in a graphite die, without special protective atmosphere at temperature of 1000°C and applied pressure of 27 MPa during 30 min [13]. Sintered samples were of cylinder form and after polishing with diamond abrasive suspension of 9, 3 and 1 μm their diameter and height were 10 mm and 4 mm, correspondingly.

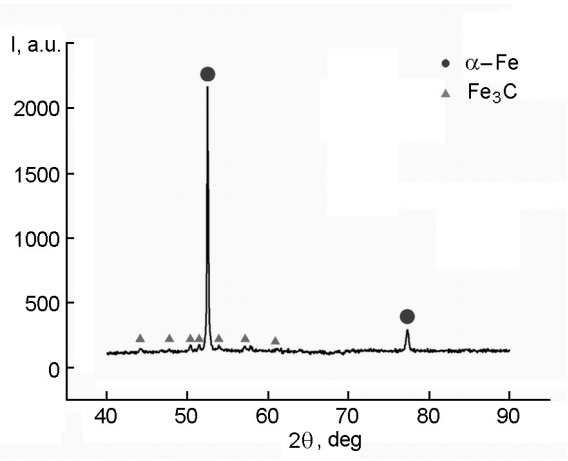

Fig. 1. Sample 6 (1 % Y_2O_3) X-ray diffractometry.

Table. Yttrium oxide content

No.	Y_2O_3 content, wt. %
1	0
2	0.1
3	0.3
4	0.5
5	0.7
6	1

The bulk densities of obtained materials were measured using the Archimedes method and for all the samples ranged between 97–99 %. Microhardness HV measurements with a Vickers indenter were performed with load of 150 g for 10 s exposure on the polished surfaces [14]. Crystalline phases in the hot-pressed specimens were determined by X-ray diffractometry (DRON-4M, St. Petersburg, Russia).

For the purpose of material crystalline structure investigation a half of each sample polished surface was etched with 10 % nitric acid solution for 20 s. The surfaces were investigated with optic microscopy (Carl Zeiss Axio Observer A1m), SEM and SEM-EDX (Teskan MIRA3).

3. Results and discussion

X-ray diffractometry of the hot-pressed composites depicted in Fig. 1 indicates the presence of α-Fe with 12 wt. % of Fe_3C which corresponded to carbon content of 0.8 wt. % in carbonyl iron powder. Absence of yttrium oxide peaks oin the XR-pattern (Fig. 1) can be explained by its little amount and low grain size.

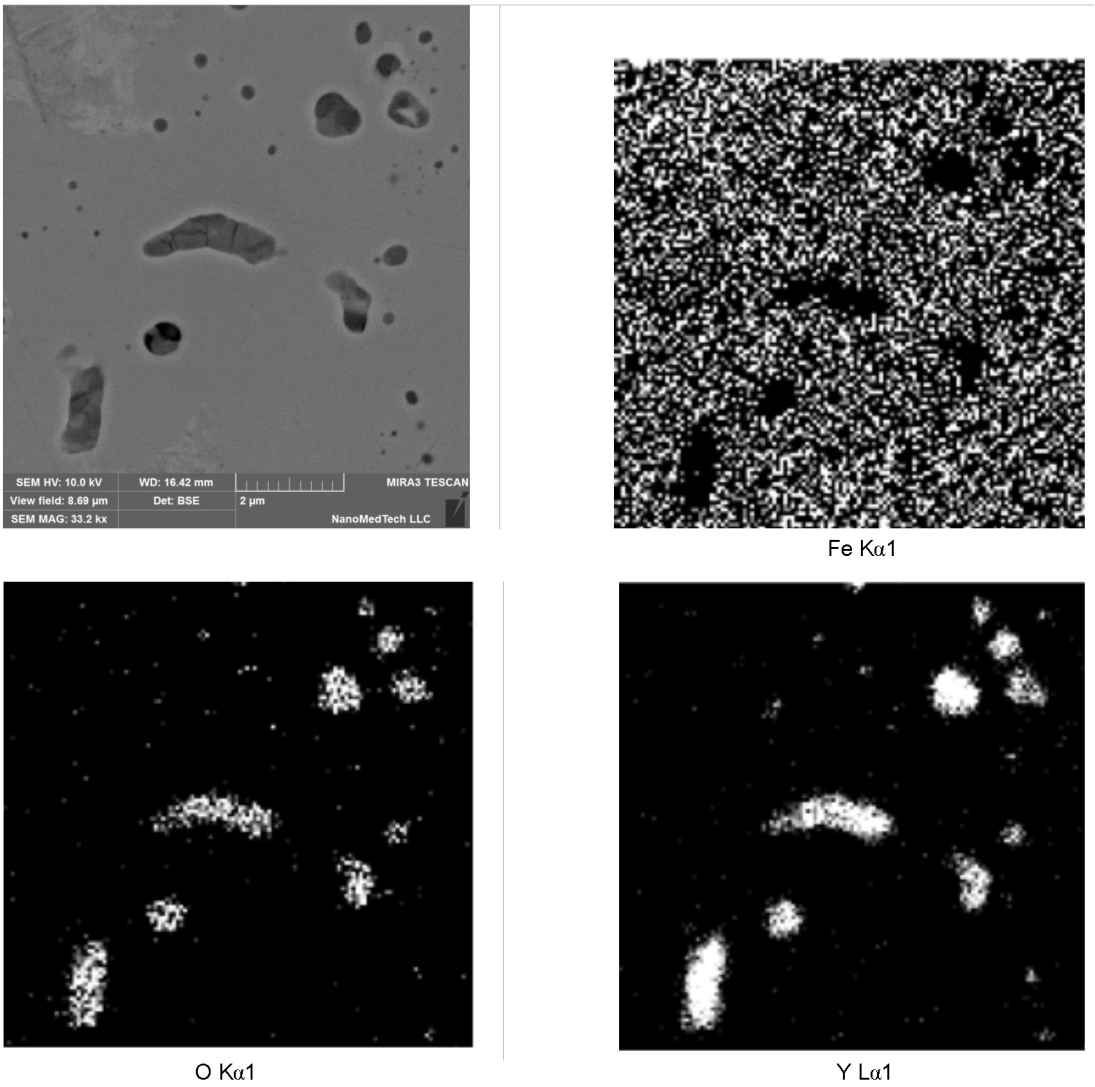

Fig. 2. Sample 6 (1 % Y_2O_3) EDX analyses.

Distribution of oxygen and yttrium atoms on sample 6 surface (Fig. 2) shows however that Y_2O_3 did not dissolve during hot pressing and remained as partially agglomerated clusters of 100–500 nm in iron-based matrix which correlates with the data of [15].

Figure 3 represents optical microscopy of the sample 6 etched surface. Here we can distinguish two different areas: "dark" and "light". Based on the data shown in [16, 17] it is clear that sintered materials have pearlitic ferrite structure typical for steels with ~ 0.8 % of carbon. Investigation of the different composition sample etched surfaces (Fig. 4) showed that yttrium oxide particles alter the matrix structure significantly: ferrite grains change their needle-like form into globular one with oxide content increasing. So yttrium oxide particles slow down ferrite needle growth leading to almost equiaxial (with the lower specific surface) grain formation.

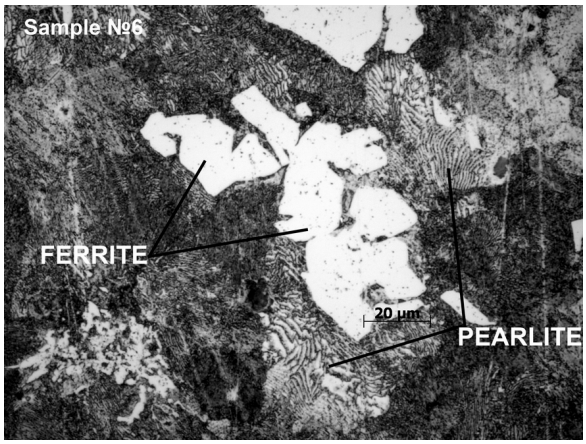

Fig. 3. Sample 6 (1 % Y_2O_3) etched surface microstructure.

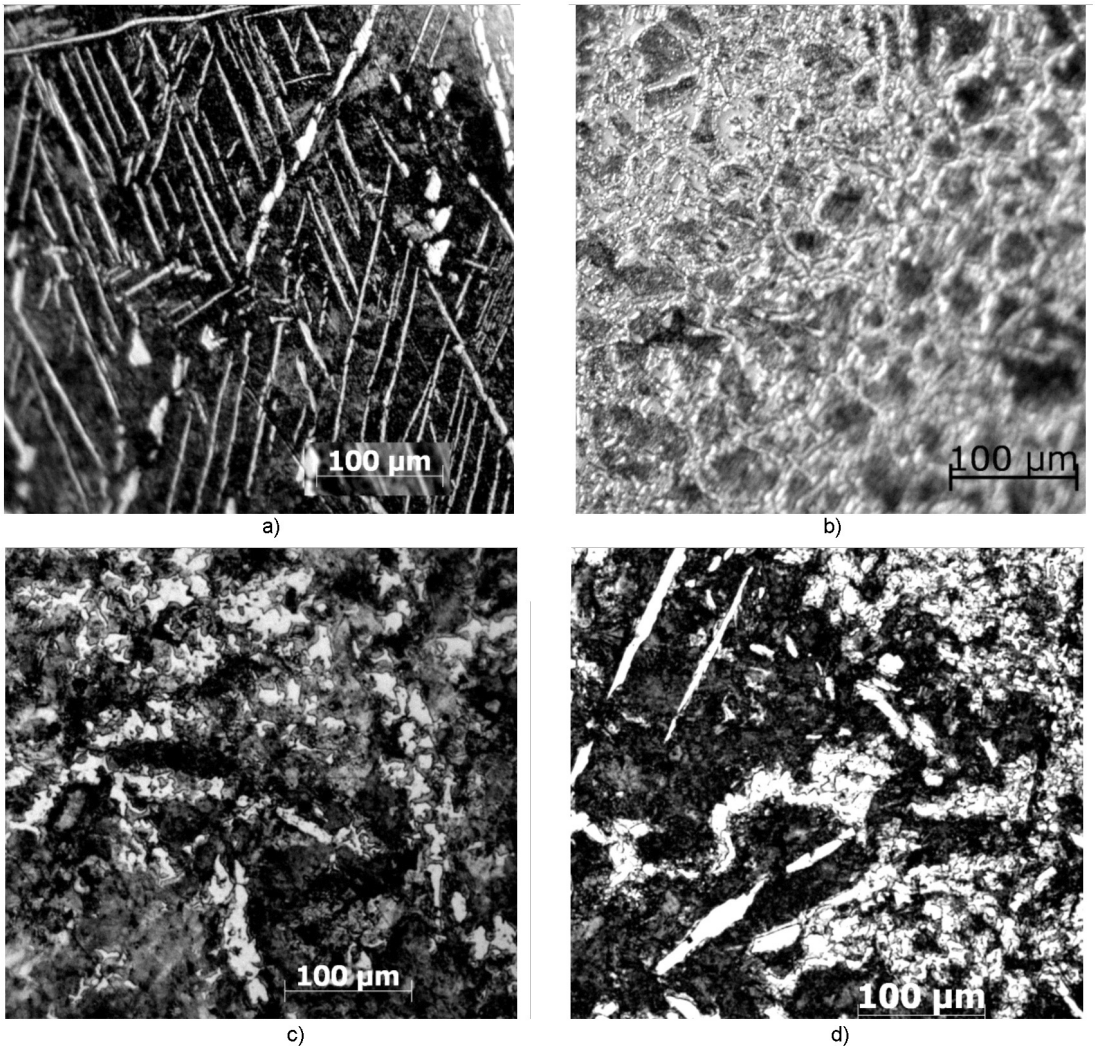

Fig. 4. Optical microscopy of matrix structure with different yttrium oxide content (a — No. 1 (0 % Y_2O_3); b — No. 3 (0.3 % Y_2O_3); c — No. 4 (0.5 % Y_2O_3); d — No. 6 (1 % Y_2O_3).

Sample 1 (which is actually pure matrix) microhardness agrees within error with the value of 2.3 GPa (Fig. 5) which can be calculated assuming the rule of mixtures and basing on the microhardness values of ferrite (2.1 GPa) and perlite (2.6 GPa) [16]. According to Fig. 5 even 1/10 percent of yttrium oxide addition strengthens the material by 21 %. Further increasing of the Y_2O_3 content to 1 % causes the microhardness enhancement up to 3.6 GPa.

It is well known [18] that microhardness of unhardened hypoeutectic steels of different structures reaches not more than 2.75 GPa. Thus, the strengthening shown in Fig. 5 cannot be explained with matrix structural evolution and should be considered to be caused by appearance of yttrium oxide clusters which delay dislocation movement [4].

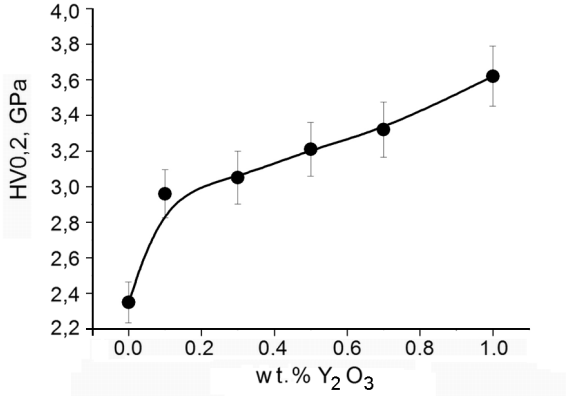

Fig. 5. The dependence of microhardness on yttrium oxide content.

The authors of [19] showed that there are several possible mechanisms of interaction of the dislocations with clusters. The authors considered two main characteristics

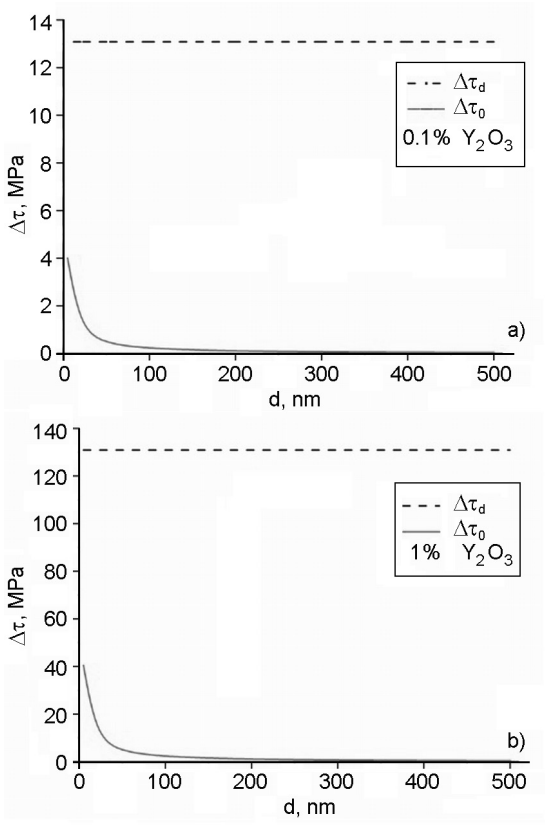

Fig. 6. Dependences of internal stress level needed for cluster destruction ($\Delta\tau_d$) and maximum additional inner stress caused with the nearby dislocation ($\Delta\tau_0$) on particle size (d); a — 0.1 % Y_2O_3; b — 1 % Y_2O_3.

of the interaction: internal stress level needed for cluster destruction ($\Delta\tau_d$) and maximum additional inner stress caused with the nearby dislocation ($\Delta\tau_0$). The mechanism is defined by the comparison of $\Delta\tau_0$ and $\Delta\tau_d$ values which can be estimated as [20]:

$$\Delta\tau_d = \frac{\pi\gamma d}{bD}, \quad (1)$$

$$\Delta\tau_0 = \frac{Cb_0}{D-d}, \quad (2)$$

were γ — cluster surface energy, D — average distance between two clusters, d — average diameter of the circle forming after cluster destruction, G — matrix phase rigidity modulus, b and b_0 — inclusion and matrix dislocation Burgers vectors correspondingly. Considering $d/D \approx \xi$ (ξ — volume fraction of inclusions) we can have:

$$\Delta\tau_d = \frac{\pi\gamma\xi}{b}, \quad (3)$$

$$\Delta\tau_0 = \frac{Cb_0}{d\left(\frac{1}{\xi}-1\right)}. \quad (4)$$

Results of the estimation with (3) and (4) using appropriate parameters for the steel matrix and yttrium oxide particles ($\gamma \approx 2.21$ J/m^2 [21], $b \approx 0.53$ nm [22], $G = 84$ GPa [23], $b_0 \approx 0.25$ nm, $D \approx 2$ μm, $d \approx 200$ nm (see Fig. 2) shown in Fig. 6 proved that dislocations overcome oxide inclusions by the Orowan mechanism which correlate with the data of [20].

4. Conclusions

Sintering of carbonyl iron-Y_2O_3 powder mixtures at 1000°C and 27 MPa during 30 min leads to composite formation with pearlitic ferrite matrix and yttrium oxide nanoinclusions. It is shown that the oxide inclusions slow down ferrite grain growth causing specific area of the phase decreasing by altering the grain shape from needle-like to globular. Increasing of Y_2O_3 content to 1 % leads to composite microhardness enhancement up to 3.6 GPa which can be explained by retardation of dislocations on disperse particles by the Orowan mechanism.

References

1. R.Gao, T.Zhang, H.L.Ding et al., *J. Nucl. Mater.*, **465**, 268 (2015).
2. R.Lindau, A.Moslang, M.Schirra et al., *J. Nucl. Mater.*, **307**, 769 (2002).
3. V.V.Brik, V.N.Voevodin, A.S.Kalchenko et al., *Probl. Sci. Tech.*, **2(84)**, 22 (2013).
4. J.Brodrick, D.J.Hepburn, G.J.Ackland, *J. Nucl. Mater.*, **445**, 291 (2014).
5. E.Cayron, I.Rath, S.Chu, C.Launois, *J. Nucl. Mater*, **335**, 83 (2004).
6. V.N.Voevodin, V.I.Karas, A.O.Komarov et al., *Probl. Sci. Tech.*, **6**, 157 (2011).
7. V.V.Svetukhin, O.G.Sidorenko, *University Proc., Volga Region, Phys. and Math. Sci.*, **2**, 49 (2007).
8. A.M.Parshin, *Probl. at Sci. Tech.*, **4**, 20 (1980).
9. Y.C.Cai, R.P.Liu, Y.H.Wei, Z.G.Cheng, *Mater. Design*, **62**, 83 (2014).
10. Z.Oksiuta, M.Lewandowska, P.Unifantowicz et al., *Fusion Eng. Des.*, **86**, 2417 (2011).
11. D.Sakuma, S.Yamashita, K.Oka et al., *J. Nucl. Mater.*, **329–333**, 392 (2004).
12. R.Schaublin, A.Ramar, N.Baluc et al., *J. Nucl. Mater.*, **351**, 247 (2006).

13. V.I.Solomonov, V.V.Osipov, V.A.Shitov, K.E.Lukjashin, *News Instit High Educat, Phys.*, **1/3**, 224 (2001).
14. V.I.Moschenok, N.A.Lalazarova, O.N.Timchenko, *Bull. Kharkov National Automobile and Highway University*, **42**, 83 (2008).
15. K.Kitayama, M.Sakaguchi, Y.Takahara, *J. Solid. State. Chem.*, **177**, 1933 (2004).
16. A.P.Gulyaev, Metal Science. Mechanical Engineering, Moscow (1986) [in Russian].
17. P.A.Vityaz et al., Powder Materials Based on Iron and Copper, Atlas Structures, Powder Metallurgy Institute, The Belarusian Science, Minsk (2008) [in Russian].
18. J.P.Kaushis, Manufacturing Processes, PHI Private Limited, New Delhi (2010).
19. K.M.Islamkulov, G.T.Aimenov, D.U.Smagulov, in: Conference Proc., Adv. Modern Nature Sci. Rec., vol.10 (2014), p.73.
20. D.V.Leleko, G.N.Tregubenko, G.A.Poliakov, *Metallurgy*, **1**, 36 (2014).
21. G.Triantafyllou, G.N.Angelopoulos, P.Nikolopoulos, *J. Mater. Sci.*, **45**, 2015 (2010).
22. R.Gaboriaud, M.Boisson, *J. de Phys. Colloques*, **41**, 171 (1980).
23. N.M.Beliaev, Strength of Materials, Science, Moscow (1965) [in Russian].